PSFC/JA-01-9

Stability of the Envelope Evolution of a Cold-Fluid Corkscrewing Elliptic Beam in a Uniform-Focusing Magnetic Field

V. Roytershteyn, C. Chen and R. Pakter

April 2001

Plasma Science and Fusion Center
Massachusetts Institute of Technology
Cambridge, MA 02139, USA

This work was supported by the Department of Energy, Office of High Energy and Nuclear Physics Grant No. DE-FG02-95ER-40919, and in part by the Department of Energy through a subcontract with Princeton Plasma Physics Laboratory. Reproduction, translation, publication, use and disposal, in whole or part, by or for the United States government is permitted.

Submitted for publication in *Physical Review E.*

Stability of the Envelope Evolution of a Cold-Fluid Corkscrewing Elliptic Beam in a Uniform-Focusing Magnetic Field

V. Roytershteyn, C. Chen and R. Pakter [1]
Plasma Science and Fusion Center
Massachusetts Institute of Technology
Cambridge, Massachusetts 02139

ABSTRACT

The envelope oscillations of a cold-fluid corkscrewing elliptic beam in a uniform-focusing magnetic field are studied. In particular, by linearizing the generalized beam envelope equations, the eigenmodes of small-amplitude envelope oscillations are calculated for a cold-fluid corkscrewing elliptic beam oscillating about its equilibrium. All of the eigenmodes are shown to be stable.

PACS: 29.27.-a, 41.75.-i, 41.85.-p

[1]Permanent address: Instituto de Fisica, Universidade Federal do Rio Grande do Sul, P.O.Box 15051, 91501-970, Porto Alegre, RS, Brazil.

I. INTRODUCTION

High-intensity charged-particle beams are widely used in basic scientific research and industries [1,2]. One important aspect in the research and development of high-intensity beams is the determination of the equilibrium and stability properties of such systems. For the simplest focusing configuration with an applied uniform-focusing magnetic field, it is well known [3] that there exist a wide variety of azimuthally symmetric beam equilibria in which beams propagate axially along the applied magnetic field and rotate azimuthally with certain internal flow velocity profiles. Some of these equilibria are stable in the context of collisionless non-neutral plasmas [3,4]. Recently, it has been shown [5,6] that in this focusing configuration, there also exists a new class of cold-fluid corkscrewing elliptic beam equilibria. In the cold-fluid corkscrewing elliptic beam equilibrium, the transverse beam cross-section is elliptic, and it rotates as the beam propagates along the applied magnetic field. The internal flow velocity profile is a combination of both the elliptical-like rotating flow and quadrupole-like flow. Applications of corkscrewing elliptic beams include beam manipulations [7,8] such as orienting beam ellipses at the interaction point in a high-energy collider [9] or at a heavy ion fusion target [10].

In this paper, we analyze the envelope oscillations of a cold-fluid corkscrewing elliptic beam about its equilibrium in a uniform-focusing magnetic field. In particular, by linearizing the generalized beam envelope equations, we determine the eigenmodes of small-amplitude envelope oscillations of a cold-fluid corkscrewing elliptic beam about its equilibrium, and show that all of the eigenmodes are stable.

The organization of this paper is as follows. In Sec. II, we present an alternative representation for the generalized beam envelope equations governing a cold-fluid corkscrewing elliptic beam equilibrium for an intense charged-particle beam propagating in a linear focusing channel consisting of solenoidal and quadrupole magnets. In Sec. III, we specialize to the case where only a uniform-focusing magnetic field is present, obtain two branches of equilibrium solutions to the beam envelope equations, and study the equilibrium flow characteristics in both branches. In Sec. IV, we carry out a linear analysis of the perturbations about the equilibrium solutions, determine the eigenmodes of small-amplitude envelope oscillations of a cold-fluid corkscrewing elliptic beam about

its equilibrium, and compare with results of the numerical integration of the generalized envelope equations. Conclusions are drawn in Sec. V.

II. GENERALIZED BEAM ENVELOPE EQUATIONS

In this section, we review cold-fluid corkscrewing elliptical beam equilibria discovered recently [5,6] and present an alternative representation of the generalized beam envelope equation. For present purposes, we consider a thin, continuous, ultrahigh-brightness, space-charge-dominated beam propagating with constant axial velocity $\beta_b c\hat{\mathbf{e}}_z$ through a linear focusing channel with multiple periodic solenoidal and alternating-gradient quadrupole focusing sections. Here, c is the speed of light in vacuum. The focusing fields can be tapered, and the quadrupoles are allowed to be at various angles in the transverse direction. The focusing magnetic field is approximated by

$$\mathbf{B}_0(\mathbf{x}) = B_z(s)\hat{\mathbf{e}}_z - \frac{1}{2}B_z'(s)\left(x\hat{\mathbf{e}}_x + y\hat{\mathbf{e}}_y\right) + \left(\partial B_{\bar{x}}^q/\partial\bar{y}\right)_0\left(\bar{y}\,\hat{\mathbf{e}}_{\bar{x}} + \bar{x}\,\hat{\mathbf{e}}_{\bar{y}}\right), \qquad (1)$$

where $B_z'(s) = \left(\partial B_z/\partial s\right)_0$, $s = z$ is the axial coordinate, $\bar{x}$, $\bar{y}$, $\hat{\mathbf{e}}_{\bar{x}}$, and $\hat{\mathbf{e}}_{\bar{y}}$ are coordinates and unit vectors of a frame of reference that is rotated by an angle of φ_q with respect to the x-axis in the laboratory frame, $\left(\P B_{\bar{x}}^q/\P\,\bar{y}\right)_0 = \left(\P B_{\bar{y}}^q/\P\,\bar{x}\right)_0$, and the subscript 'zero' denotes $(x,y) = 0 = (\bar{x},\bar{y})$.

It has been shown in the paraxial approximation that there exists a class of solutions to steady-state cold-fluid equations [5,6], which, in general, describes corkscrewing elliptic beam equilibria for ultrahigh-brightness, space-charge-dominated beam propagating through the applied focusing magnetic field defined in Eq. (1). The generalized beam envelope equations are [5,6]

$$\frac{d^2a}{ds^2} + \left(\kappa_q(s)\cos\left[2(\theta-\varphi_q)\right] - \frac{b^2\left(\alpha_x^2 - 2\alpha_x\alpha_y\right) + a^2\alpha_y^2}{a^2-b^2} - 2\alpha_y\sqrt{\kappa_z(s)}\right)a - \frac{2K}{a+b} = 0, \qquad (2)$$

$$\frac{d^2b}{ds^2} - \left(\kappa_q(s)\cos\left[2(\theta-\varphi_q)\right] - \frac{a^2\left(\alpha_y^2 - 2\alpha_x\alpha_y\right) + b^2\alpha_x^2}{a^2-b^2} + 2\alpha_x\sqrt{\kappa_z(s)}\right)b - \frac{2K}{a+b} = 0, \qquad (3)$$

$$\frac{1}{b}\frac{d}{ds}\left\{b^2\left[\alpha_x + \sqrt{\kappa_z(s)}\right]\right\} - \frac{a^3\left(\alpha_x - \alpha_y\right)}{a^2-b^2}\frac{d}{ds}\left(\frac{b}{a}\right) + \kappa_q(s)b\sin\left[2(\theta-\varphi_q)\right] = 0, \qquad (4)$$

$$\frac{1}{a}\frac{d}{ds}\left\{a^2\left[\alpha_y+\sqrt{\kappa_z(s)}\right]\right\}-\frac{b^3\left(\alpha_x-\alpha_y\right)}{a^2-b^2}\frac{d}{ds}\left(\frac{a}{b}\right)-\kappa_q(s)a\sin\left[2\left(\theta-\varphi_q\right)\right]=0, \tag{5}$$

$$\frac{d\theta}{ds}-\frac{a^2\alpha_y-b^2\alpha_x}{a^2-b^2}=0. \tag{6}$$

In Eqs. (2)-(6), $\sqrt{\kappa_z(s)}=qB_z(s)/2\gamma_b\beta_b mc^2$ is the focusing parameter for the uniform-focusing magnetic field, $K=2q^2N_b/\gamma_b^3\beta_b^2mc^2$ is the normalized self-field perveance, and the variables $a(s)$, $b(s)$, $\alpha_x(s)$, $\beta_x(s)$ and $\theta(s)$ specify the density and flow velocity of the cold-fluid corkscrewing elliptic beam equilibrium as defined in Refs. 5 and 6. Here, m and q are the rest mass and charge of the particle, N_b is the number of particles per unit axial length, and $\gamma_b=\left(1-\beta_b^2\right)^{-1/2}$ is the relativistic mass factor.

It proves to be convenient to transform Eqs. (2)-(6) to a more symmetric form by introducing new variables

$$x_1=a+b, \tag{7}$$

$$x_2=aa_y+ba_x, \tag{8}$$

$$x_3=\frac{dx_1}{ds} \tag{9}$$

$$x_4=a-b, \tag{10}$$

$$x_5=aa_y-ba_x, \tag{11}$$

$$x_6=\frac{dx_4}{ds}. \tag{12}$$

Adding Eqs. (2) and (3) and subtracting Eq. (3) from Eq. (2) yields

$$\frac{d^2x_1}{ds^2}+x_4\kappa_q(s)\cos\left[2\left(\theta-\varphi_q\right)\right]-2x_2\sqrt{\kappa_z(s)}-\frac{4K}{x_1}-\frac{x_2^2}{x_1}=0, \tag{13}$$

$$\frac{d^2x_4}{ds^2}+x_1\kappa_q(s)\cos\left[2\left(\theta-\varphi_q\right)\right]-2x_5\sqrt{\kappa_z(s)}-\frac{x_5^2}{x_4}=0, \tag{14}$$

respectively. Similarly, adding Eqs. (4) and (5) and subtracting Eq. (5) from Eq. (4) yields

$$\frac{dx_2}{ds}+x_1\frac{d}{ds}\sqrt{\kappa_z(s)}+2\sqrt{\kappa_z(s)}\frac{dx_1}{ds}+\frac{x_2}{x_1}\frac{dx_1}{ds}-\kappa_q(s)x_4\sin\left[2\left(\theta-\varphi_q\right)\right]=0, \tag{15}$$

$$\frac{dx_5}{ds} + x_4 \frac{d}{ds}\sqrt{\kappa_z(s)} + 2\sqrt{\kappa_z(s)}\frac{dx_4}{ds} + \frac{x_5}{x_4}\frac{dx_4}{ds} - \kappa_q(s)x_1 \sin\left[2\left(\theta - \varphi_q\right)\right] = 0, \tag{16}$$

Finally, Eq. (6) can be expressed in terms of the new variables as

$$\frac{d}{ds}\theta - \frac{x_1 x_5 + x_2 x_4}{2x_1 x_4} = 0. \tag{17}$$

Furthermore, it is convenient to express Eqs. (13)–(16) in terms of the following first-order differential equations:

$$\frac{dx_1}{ds} = x_3, \tag{18}$$

$$\frac{dx_2}{ds} = -x_1 \frac{d}{ds}\sqrt{\kappa_z(s)} - 2x_3\sqrt{\kappa_z(s)} - \frac{x_2 x_3}{x_1} + \kappa_q(s)x_4 \sin\left[2\left(\theta - \varphi_q\right)\right], \tag{19}$$

$$\frac{dx_3}{ds} = 2x_2\sqrt{\kappa_z(s)} + \frac{4K}{x_1} + \frac{x_2^2}{x_1} - \kappa_q(s)x_4 \cos\left[2\left(\theta - \varphi_q\right)\right], \tag{20}$$

$$\frac{dx_4}{ds} = x_6, \tag{21}$$

$$\frac{dx_5}{ds} = -x_4 \frac{d}{ds}\sqrt{\kappa_z(s)} - 2x_6\sqrt{\kappa_z(s)} - \frac{x_5 x_6}{x_4} + \kappa_q(s)x_1 \sin\left[2\left(\theta - \varphi_q\right)\right], \tag{22}$$

$$\frac{dx_6}{ds} = 2x_5\sqrt{\kappa_z(s)} + \frac{x_5^2}{x_4} - \kappa_q(s)x_1 \cos\left[2\left(\theta - \varphi_q\right)\right]. \tag{23}$$

In general, Eqs. (17)-(23) must be solved simultaneously. In circumstances where only solenoidal magnetic fields are present, i.e., for $\kappa_q(s) = 0$ and $\kappa_z(s) \neq 0$, the system defined in Eqs. (18)-(23) decouples into two independent systems with (x_1, x_2, x_3) and (x_4, x_5, x_6), respectively, and the angle θ becomes a slaved variable and can be integrated from Eq. (17).

III. SOLUTION TO THE BEAM ENVELOPE EQUATIONS

For a uniform-focusing magnetic field with $\kappa_q(s) = 0$ and $\kappa_z(s) = \kappa_{z0} = \text{const.}$, Eqs. (18)-(23) split into two sets of uncoupled equations, and the variable θ becomes a slaved variable that can be integrated from Eq. (17). Equations (18)-(20) for (x_1, x_2, x_3) describe symmetric modes with the envelopes a and b oscillating in phase, whereas Eqs. (21)-

(23) for (x_4, x_5, x_6) describe anti-symmetric modes with the envelopes a and b oscillating with opposite phase.

The steady-state solutions to Eqs. (18)-(23) can be obtained analytically. Two branches of physically acceptable special solutions are:

$$x_1 = -\frac{4K + x_2^2}{2x_2\sqrt{\kappa_{z0}}} = \text{const.},\ x_4 = \text{const.},\ \text{and}\ x_3 = x_5 = x_6 = 0 \tag{24}$$

for branch A, and

$$x_1 = -\frac{4K + x_2^2}{2x_2\sqrt{\kappa_{z0}}} = \text{ const.},\ x_4 = -\frac{x_5}{2\sqrt{\kappa_{z0}}} = \text{const., and}\ x_3 = x_6 = 0 \tag{25}$$

for branch B.

It is interesting to point out that these solutions represent two different types of equilibrium flow. Indeed, according to Refs. 5 and 6, the equilibrium beam density and flow velocity are given by

$$n_b(\mathbf{x}_\perp, s) = \frac{N_b}{p\, a(s) b(s)} \Theta\left[1 - \frac{\tilde{x}^2}{a^2(s)} - \frac{\tilde{y}^2}{b^2(s)}\right], \tag{26}$$

$$\mathbf{V}_\perp(\mathbf{x}_\perp, s) = -\alpha_x(s)\tilde{y}\beta_b c\hat{\mathbf{e}}_{\tilde{x}} + \alpha_y(s)\tilde{x}\beta_b c\hat{\mathbf{e}}_{\tilde{y}}, \tag{27}$$

where $\Theta(x) = 1$ if $x > 0$ and $\Theta(x) = 0$ if $x < 0$,

$$\tilde{x} = x\cos\theta(s) + y\sin\theta(s), \tag{28}$$

$$\tilde{y} = -x\sin\theta(s) + y\cos\theta(s), \tag{29}$$

and $\theta(s)$ is a solution to Eq. (17). Making use of the definitions in Eqs. (8) and (11), we can express the equilibrium velocity as

$$\frac{\mathbf{V}_\perp(\mathbf{x}_\perp, s)}{\beta_b c} = \frac{x_2}{2}\left(\frac{\tilde{x}}{a}\hat{\mathbf{e}}_{\tilde{y}} - \frac{\tilde{y}}{b}\hat{\mathbf{e}}_{\tilde{x}}\right) + \frac{x_5}{2}\left(\frac{\tilde{y}}{b}\hat{\mathbf{e}}_{\tilde{x}} + \frac{\tilde{x}}{a}\hat{\mathbf{e}}_{\tilde{y}}\right). \tag{30}$$

In Eq. (30), the first term represents elliptical-like rotation, whereas the second term describes quadrupole-like flow. Therefore x_2 and x_5 can be considered as measures of elliptical-like rotation and quadrupole-like flow, respectively. For branch A, $x_5 = 0$, and the corresponding flow is pure elliptical-like rotation. Branch B is a mixture of both elliptical-like rotation and quadrupole-like flow because both x_2 and x_5 are nonzero.

Making use of the definitions in Eqs. (7)-(12), it is possible to solve the envelope functions a and b in terms of the parameters a_x and a_y from Eqs. (24) and (25). This gives

$$a = \sqrt{\frac{\alpha_x}{\alpha_y}}\left[\frac{K}{\kappa_{z0} - \left(\alpha_x + \sqrt{\kappa_{z0}}\right)\left(\alpha_y + \sqrt{\kappa_{z0}}\right)}\right]^{1/2} \tag{31}$$

$$b = \sqrt{\frac{\alpha_y}{\alpha_x}}\left[\frac{K}{\kappa_{z0} - \left(\alpha_x + \sqrt{\kappa_{z0}}\right)\left(\alpha_y + \sqrt{\kappa_{z0}}\right)}\right]^{1/2} \tag{32}$$

for branch A, and

$$a = \sqrt{\frac{\alpha_x + 2\sqrt{\kappa_{z0}}}{\alpha_y + 2\sqrt{\kappa_{z0}}}}\left[\frac{K}{\kappa_{z0} - \left(\alpha_x + \sqrt{\kappa_{z0}}\right)\left(\alpha_y + \sqrt{\kappa_{z0}}\right)}\right]^{1/2} \tag{33}$$

$$b = \sqrt{\frac{\alpha_y + 2\sqrt{\kappa_{z0}}}{\alpha_x + 2\sqrt{\kappa_{z0}}}}\left[\frac{K}{\kappa_{z0} - \left(\alpha_x + \sqrt{\kappa_{z0}}\right)\left(\alpha_y + \sqrt{\kappa_{z0}}\right)}\right]^{1/2} \tag{34}$$

for branch B. In both cases, a_x and a_y are constant. The conditions for the confinement of corkscrewing elliptic beam equilibria are

$$\alpha_x/\sqrt{\kappa_{z0}} > -2,\ \alpha_y/\sqrt{\kappa_{z0}} > -2 \text{ and } \left(1+\alpha_x/\sqrt{\kappa_{z0}}\right)\left(1+\alpha_y/\sqrt{\kappa_{z0}}\right) < 1. \tag{35}$$

In the special case with $\alpha_x = \alpha_y$, the beam becomes round, recovering the well-known rigid-rotor equilibrium [3,4].

IV. STABILITY ANALYSIS

To determine the stability properties of the steady-state solutions in Eqs. (24) and (25) or Eqs. (31)-(33), we linearize equations (18)-(23) to obtain

$$\frac{d\mathbf{dx}}{ds} = \mathbf{A}\cdot\mathbf{dx}, \tag{36}$$

where $\mathbf{dx} = (dx_1, dx_2, ..., dx_6)^{\mathrm{T}}$ and $\mathbf{A}$ is a 6×6 matrix with the following non-zero elements:

$$A_{13}=1,\ A_{23}=-2\sqrt{\kappa_{z0}}-\frac{x_2}{x_1},\ A_{31}=-\frac{4K}{x_1^2}-\frac{x_2^2}{x_1^2},\ A_{32}=2\sqrt{\kappa_{z0}}+\frac{2x_2}{x_1},\ A_{46}=1,$$

$$A_{56}=-2\sqrt{\kappa_{z0}}-\frac{x_5}{x_4},\ A_{64}=-\frac{x_5^2}{x_4^2},\text{ and }\ A_{65}=2\sqrt{\kappa_{z0}}+\frac{2x_5}{x_4}. \tag{37}$$

For the steady-state solutions in Eqs. (24) and (25) or Eqs. (31)-(34) to be stable, all of the eigenvalues of $\mathbf{A}$, $\{l_i\}$, must satisfy the condition $Re(\lambda_i)=0$, where $i=1,2,\cdots,6$.

A. Eigenvalues for Branch A

For branch A, the eigenvalue equation $\det(\mathbf{A}-l\mathbf{I})=0$ can be expressed as

$$\lambda^2\left(\lambda^2+4\kappa_{z0}\right)\left\{\left(\alpha_x+\alpha_y\right)^2\lambda^2+4\left(\alpha_x^2+\alpha_y^2\right)\kappa_{z0}+8\alpha_x\alpha_y\left[\alpha_x\alpha_y+\kappa_{z0}+\left(\alpha_x+\alpha_y\right)\sqrt{\kappa_{z0}}\right]\right\}=0. \tag{38}$$

Therefore, the eigenvalues are:

$$\begin{aligned}\lambda_{1,2}&=0\\ \lambda_{3,4}&=\pm2\sqrt{\kappa_{z0}}\,i\\ \lambda_{5,6}&=\pm2\sqrt{\kappa_{z0}}\,\frac{\sqrt{F_A}}{\hat{\alpha}_x+\hat{\alpha}_y}i\end{aligned} \tag{39}$$

where $F_A=\left(\hat{\alpha}_x+\hat{\alpha}_y+\hat{\alpha}_x\hat{\alpha}_y\right)^2+\hat{\alpha}_x^2\hat{\alpha}_y^2$, $\hat{\alpha}_x=\alpha_x/\sqrt{\kappa_{z0}}$ and $\hat{\alpha}_y=\alpha_y/\sqrt{\kappa_{z0}}$. It is readily shown that the function F_A has only one real root and therefore is always greater or equal to zero, i.e., $F_A\geq0$. Consequently, all of the eigenvalues in Eq. (39) satisfy the condition $\mathrm{Re}(l)=0$, which means that branch A is always stable.

A closer examination of the eigenvectors show that the eigenmodes associated with the eigenvalues λ_3 and λ_4 correspond to the envelopes a and b oscillating exactly out of phase, which we refer to as the out-of-phase eigenmode oscillations. On the other hand, the eigenmodes associated with the eigenvalues λ_5 and λ_6 correspond to the envelopes a and b oscillating exactly in phase, which we refer to as the in-phase eigenmode oscillations.

Figure 1 shows the in-phase eigenmode oscillations about an equilibrium solution in branch A, as obtained by integrating Eqs. (2)-(6) numerically. The choice of system parameters and initial conditions in Fig. 1 corresponds to: $K=5.0\times10^{-3}$,

$\alpha_x(0)/\sqrt{\kappa_{z0}} = -0.7$, $\alpha_y(0)/\sqrt{\kappa_{z0}} = -1.6$, $a(0)\sqrt{\kappa_{z0}} = 0.0431$, $b(0)\sqrt{\kappa_{z0}} = 0.0984$, and $a'(0) = b'(0) = 0.02$. Here, the equilibrium solution corresponds to: $\alpha_x(s)/\sqrt{\kappa_{z0}} = -0.7$, $\alpha_y(s)/\sqrt{\kappa_{z0}} = -1.6$, $a(s)\sqrt{\kappa_{z0}} = 0.0431$, $b(s)\sqrt{\kappa_{z0}} = 0.0984$, and $a'(s) = b'(s) = 0$. In this case, the envelopes a and b oscillate exactly in phase, but the variables α_x and α_y oscillate out of phase. The normalized frequency of the eigenmode oscillations is $|\lambda_5|/\sqrt{\kappa_{z0}} = 1.42$, which is in agreement with the expression for the eigenvalue λ_5 (or λ_6) given in Eq. (39).

Figure 2 shows the out-of-phase eigenmode oscillations about the same equilibrium solution in branch A as shown in Fig. 1, as obtained by integrating Eqs. (2)-(6) numerically. The choice of system parameters and initial conditions in Fig. 2 corresponds to: $K = 5.0\times10^{-3}$, $\alpha_x(0)/\sqrt{\kappa_{z0}} = -0.7$, $\alpha_y(0)/\sqrt{\kappa_{z0}} = -1.6$, $a(0)\sqrt{\kappa_{z0}} = 0.0431$, $b(0)\sqrt{\kappa_{z0}} = 0.0984$, and $a'(0) = -b'(0) = 0.02$. For the case shown in Fig. 2, the envelopes a and b oscillate exactly out of phase, and so do the variables α_x and α_y. The normalized frequency of the eigenmode oscillations in Fig. 3 is $|\lambda_3|/\sqrt{\kappa_{z0}} = 2.0$, which is in agreement with the expression for the eigenvalue λ_3 (or λ_4) given in Eq. (39).

B. Eigenvalues for Branch B

For branch B, the eigenvalue equation is of the form

$$\lambda^2\left(\lambda^2 + 4\kappa_{z0}\right)\left\{\left(\alpha_x + \alpha_y + 4\sqrt{\kappa_{z0}}\right)^2\lambda^2 + 5\left(\alpha_x^2 + \alpha_y^2\right)\kappa_{z0} + 16\left(\alpha_x + \alpha_y + \sqrt{\kappa_{z0}}\right)\sqrt{\kappa_{z0}^3} + 2\alpha_x\alpha_y\left[\alpha_x\alpha_y + 9\kappa_{z0} + 3\left(\alpha_x + \alpha_y\right)\sqrt{\kappa_{z0}}\right]\right\} = 0 \tag{40}$$

which yields the following eigenvalues

$$\begin{aligned} \lambda_{1,2} &= 0 \\ \lambda_{3,4} &= \pm 2\sqrt{\kappa_{z0}}\, i \\ \lambda_{5,6} &= \pm 2\sqrt{\kappa_{z0}}\,\frac{\sqrt{F_B}}{\left|\hat{\alpha}_x + \hat{\alpha}_y + 4\right|} i \end{aligned} \tag{41}$$

where $F_B = 2\hat{\alpha}_x^2\hat{\alpha}_y^2 + 6\hat{\alpha}_x^2\hat{\alpha}_y + 5\hat{\alpha}_x^2 + 6\hat{\alpha}_y^2\hat{\alpha}_x + 18\hat{\alpha}_x\hat{\alpha}_y + 16\hat{\alpha}_x + 5\hat{\alpha}_y^2 + 16\hat{\alpha}_y + 16$. The function F_B has no real roots, and therefore is always greater then zero, i.e., $F_B > 0$.

Consequently, all of the eigenvalues in Eq. (41) satisfy the condition $\mathrm{Re}(l)=0$, which means that branch B is also stable. Associated with the eigenvalues λ_3 and λ_4 in Eq. (41) are the in-phase eigenmode oscillations in which the envelopes a and b oscillate exactly in phase, whereas the eigenmodes associated with the eigenvalues λ_5 and λ_6 correspond to the out-of-phase oscillations.

Figure 3 shows the in-phase eigenmode oscillations about an equilibrium solution in branch B, as obtained by integrating Eqs. (2)-(6) numerically. The choice of system parameters and initial conditions in Fig. 3 corresponds to: $K=5.0\times10^{-3}$, $\alpha_x(0)/\sqrt{\kappa_{z0}}=-0.7$, $\alpha_y(0)/\sqrt{\kappa_{z0}}=-1.6$, $a(0)\sqrt{\kappa_{z0}}=0.117$, $b(0)\sqrt{\kappa_{z0}}=0.0361$, and $a'(0)=b'(0)=0.02$. Here, the equilibrium solution corresponds to: $\alpha_x(s)/\sqrt{\kappa_{z0}}=-0.7$, $\alpha_y(s)/\sqrt{\kappa_{z0}}=-1.6$, $a(s)\sqrt{\kappa_{z0}}=0.117$, $b(s)\sqrt{\kappa_{z0}}=0.0361$, and $a'(s)=b'(s)=0$. For this eigenmode, the envelopes a and b oscillate exactly in phase, and so do the variables α_x and α_y. The frequency of the oscillations in Fig. 3 is $|\lambda_3|/\sqrt{\kappa_{z0}}=1.52$, which is in agreement with the expression for the eigenvalue λ_3 (or λ_4) given in Eq. (41).

Figure 4 shows the out-of-phase eigenmode oscillations about the same equilibrium solution shown in Fig. 3, as obtained by integrating Eqs. (2)-(6) numerically. The choice of system parameters and initial conditions in Fig. 4 corresponds to: $K=5.0\times10^{-3}$, $\alpha_x(0)/\sqrt{\kappa_{z0}}=-0.7$, $\alpha_y(0)/\sqrt{\kappa_{z0}}=-1.6$, $a(0)\sqrt{\kappa_{z0}}=0.117$, $b(0)\sqrt{\kappa_{z0}}=0.0361$, and $a'(0)=-b'(0)=0.02$. The frequency of the oscillations in Fig. 4 is $|\lambda_5|/\sqrt{\kappa_{z0}}=2.0$, which in agreement with the expression for the eigenvalue λ_5 (or λ_6) given in Eq. (41).

V. CONCLUSION

We have analyzed the envelope oscillations of a cold-fluid corkscrewing elliptic beam in an applied uniform-focusing magnetic field. In particular, an alternative representation was presented for the generalized beam envelope equations governing a cold-fluid corkscrewing elliptic beam equilibrium for an intense charged-particle beam propagating in a linear focusing channel consisting of solenoidal and quadrupole magnets. For the case of a uniform-focusing magnetic field, two branches of equilibrium

solutions to the beam envelope equations were obtained, and the equilibrium flow characteristics in both branches were studied. A linear analysis of the perturbations about the equilibrium solutions was performed to determine the eigenmodes of small-amplitude envelope oscillations of a cold-fluid corkscrewing elliptic beam about its equilibrium. Excellent agreement was found between the eigenmode calculations and the numerical integration of the generalized envelope equations. All of the eigenmodes were shown to be stable.

ACKNOWLEDMENTS

This work was supported by the Department of Energy, Office of High Energy and Nuclear Physics Grant No. DE-FG02-95ER-40919, and in part by the Department of Energy through a subcontract with Princeton Plasma Physics Laboratory. Research by R. Pakter was also supported by CNPq, Brazil.

REFERENCES

1. *Physics of High-Brightness Beam*, edited by J. Rosenzweig and L. Sarafini (World Scientific, New York, 2001), in press.
2. *Space-Charge Dominated Beams and Application of High-Brightness Beams*, edited by S. Y. Lee, AIP Conf. Proc. No. 377 (AIP, New York, 1996).
3. R. C. Davidson, Physics of Nonneutral Plasmas (Addison-Wesley, Reading, MA, 1990).
4. R. C. Davidson and N. A. Krall, Phys. Fluids **13**, 1543 (1970).
5. R. Pakter and C. Chen, Phys. Rev. **E62**, 2789 (2000).
6. C. Chen and R. Pakter, Phys. Plasmas **7**, 2203 (2000).
7. D. Chernin, Part. Accel. **24**, 29 (1988).
8. J. J. Barnard, in Proceedings of the 1995 Particle Accelerator Conference (Institute of Electrical and Electronics Engineering, Piscataway, NJ, 1995), p. 3241.
9. R. H. Siemann, in Proceedings of the 1993 Particle Accelerator Conference (Institute of Electrical and Electronics Engineering, Piscataway, NJ, 1993), p. 532.
10. A. W. Molvik and J. J. Barnard, "Matching final focusing to distributed radiator target requirements," to appear in Proceedings of the Thirteenth International Symposium on Heavy Ion Fusion, edited by E. Lee., Nuclear Instruments and Methods in Physics Research A (2001).

FIGURE CAPTIONS

Fig. 1 Plots of the in-phase eigenmode oscillations about an equilibrium solution in branch A: (a) normalized beam envelopes $a\sqrt{\kappa_{z0}}$ and $b\sqrt{\kappa_{z0}}$ versus the normalized propagating distance $s\sqrt{\kappa_{z0}}$, and (b) normalized variables $\alpha_x/\sqrt{\kappa_{z0}}$ and $\alpha_x/\sqrt{\kappa_{z0}}$ versus the normalized propagating distance $s\sqrt{\kappa_{z0}}$. Here, the choice of system parameters and initial conditions corresponds to: $K = 5.0\times10^{-3}$, $\alpha_x(0)/\sqrt{\kappa_{z0}} = -0.7$, $\alpha_y(0)/\sqrt{\kappa_{z0}} = -1.6$, $a(0)\sqrt{\kappa_{z0}} = 0.0431$, $b(0)\sqrt{\kappa_{z0}} = 0.0984$, and $a'(0) = b'(0) = 0.02$. The equilibrium solution corresponds to: $\alpha_x(s)/\sqrt{\kappa_{z0}} = -0.7$, $\alpha_y(s)/\sqrt{\kappa_{z0}} = -1.6$, $a(s)\sqrt{\kappa_{z0}} = 0.0431$, $b(s)\sqrt{\kappa_{z0}} = 0.0984$, and $a'(s) = b'(s) = 0$.

Fig. 2 Plots of the out-of-phase eigenmode oscillations about the same equilibrium solution in branch A as shown in Fig. 1: (a) normalized beam envelopes $a\sqrt{\kappa_{z0}}$ and $b\sqrt{\kappa_{z0}}$ versus the normalized propagating distance $s\sqrt{\kappa_{z0}}$, and (b) normalized variables $\alpha_x/\sqrt{\kappa_{z0}}$ and $\alpha_x/\sqrt{\kappa_{z0}}$ versus the normalized propagating distance $s\sqrt{\kappa_{z0}}$. Here, the choice of system parameters and initial conditions corresponds to: $K = 5.0\times10^{-3}$, $\alpha_x(0)/\sqrt{\kappa_{z0}} = -0.7$, $\alpha_y(0)/\sqrt{\kappa_{z0}} = -1.6$, $a(0)\sqrt{\kappa_{z0}} = 0.0431$, $b(0)\sqrt{\kappa_{z0}} = 0.0984$, and $a'(0) = -b'(0) = 0.02$.

Fig. 3 Plots of the in-phase eigenmode oscillations about an equilibrium solution in branch B: (a) normalized beam envelopes $a\sqrt{\kappa_{z0}}$ and $b\sqrt{\kappa_{z0}}$ versus the normalized propagating distance $s\sqrt{\kappa_{z0}}$, and (b) normalized variables $\alpha_x/\sqrt{\kappa_{z0}}$ and $\alpha_x/\sqrt{\kappa_{z0}}$ versus the normalized propagating distance $s\sqrt{\kappa_{z0}}$. Here, the choice of system parameters and initial conditions corresponds to: $K = 5.0\times10^{-3}$, $\alpha_x(0)/\sqrt{\kappa_{z0}} = -0.7$, $\alpha_y(0)/\sqrt{\kappa_{z0}} = -1.6$, $a(0)\sqrt{\kappa_{z0}} = 0.117$, $b(0)\sqrt{\kappa_{z0}} = 0.0361$, and $a'(0) = b'(0) = 0.02$. The equilibrium solution corresponds to: $\alpha_x(s)/\sqrt{\kappa_{z0}} = -0.7$, $\alpha_y(s)/\sqrt{\kappa_{z0}} = -1.6$, $a(s)\sqrt{\kappa_{z0}} = 0.117$, $b(s)\sqrt{\kappa_{z0}} = 0.0361$,

and $a'(s)=b'(s)=0$.

Fig. 4 Plots of the out-of-phase eigenmode oscillations about the same equilibrium solution in branch B as shown in Fig. 3: (a) normalized beam envelopes $a\sqrt{\kappa_{z0}}$ and $b\sqrt{\kappa_{z0}}$ versus the normalized propagating distance $s\sqrt{\kappa_{z0}}$, and (b) normalized variables $\alpha_x/\sqrt{\kappa_{z0}}$ and $\alpha_x/\sqrt{\kappa_{z0}}$ versus the normalized propagating distance $s\sqrt{\kappa_{z0}}$. Here, the choice of system parameters and initial conditions corresponds to: $K=5.0\times10^{-3}$, $\alpha_x(0)/\sqrt{\kappa_{z0}}=-0.7$, $\alpha_y(0)/\sqrt{\kappa_{z0}}=-1.6$, $a(0)\sqrt{\kappa_{z0}}=0.117$, $b(0)\sqrt{\kappa_{z0}}=0.0361$, and $a'(0)=-b'(0)=0.02$.

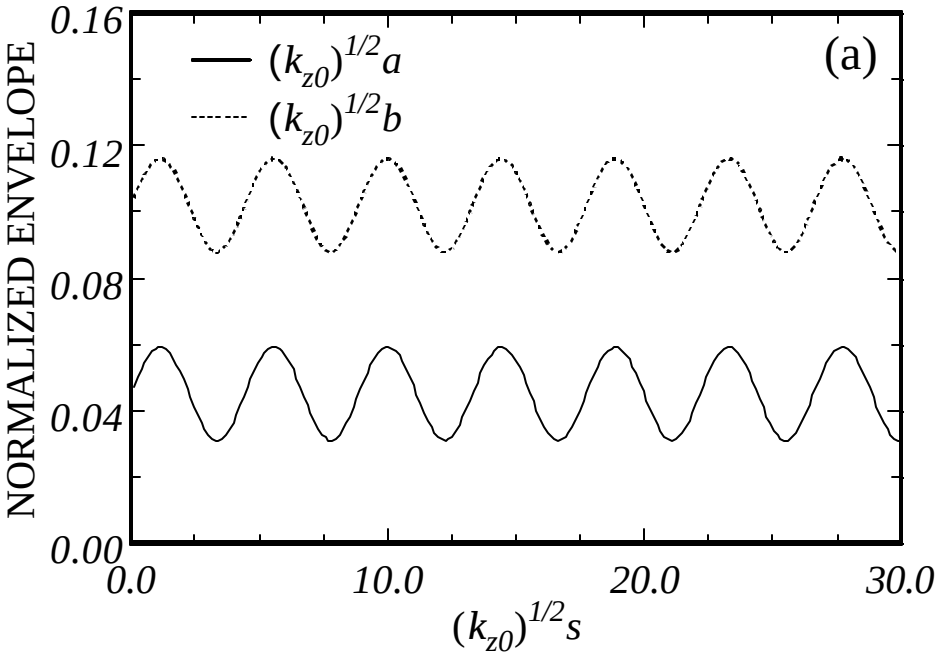
0.16
0.12
0.08
0.04
0.00
NORMALIZED ENVELOPE
$(k_{z0})^{1/2}a$
$(k_{z0})^{1/2}b$
(a)
0.0
10.0
20.0
30.0
$(k_{z0})^{1/2}s$

Fig. 1(a)

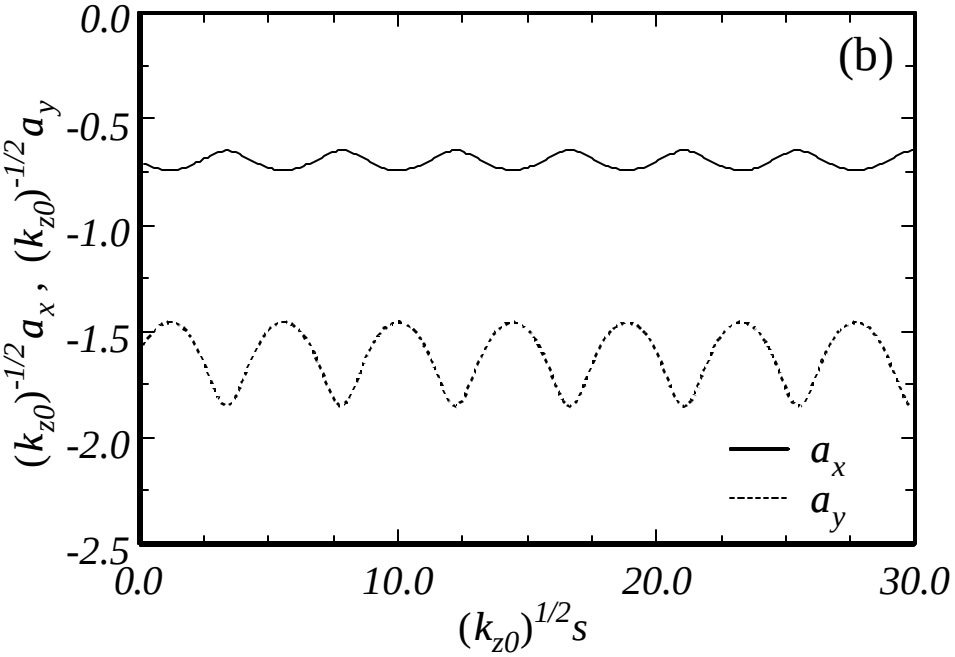

Fig. 1(b)

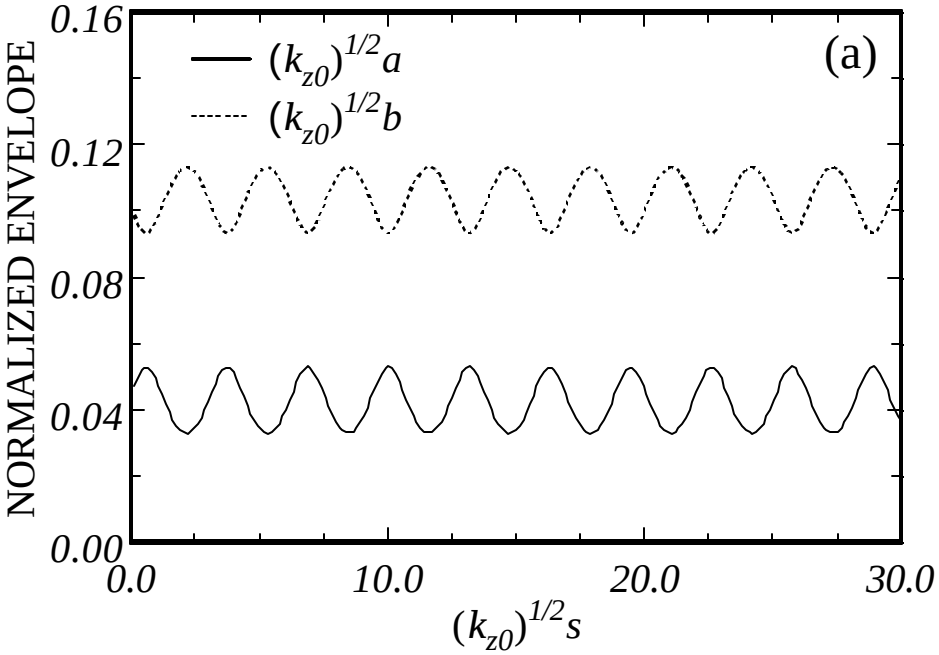
0.16
0.12
0.08
0.04
0.00
NORMALIZED ENVELOPE
$(k_{z0})^{1/2}a$
$(k_{z0})^{1/2}b$
(a)
0.0
10.0
20.0
30.0
$(k_{z0})^{1/2}s$

Fig. 2(a)

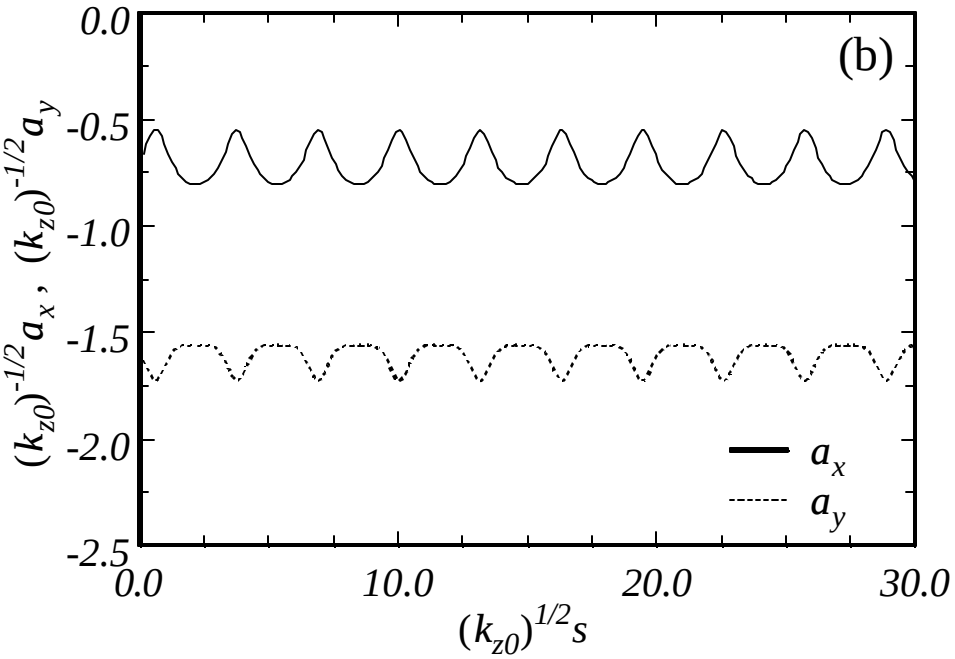

Fig. 2(b)

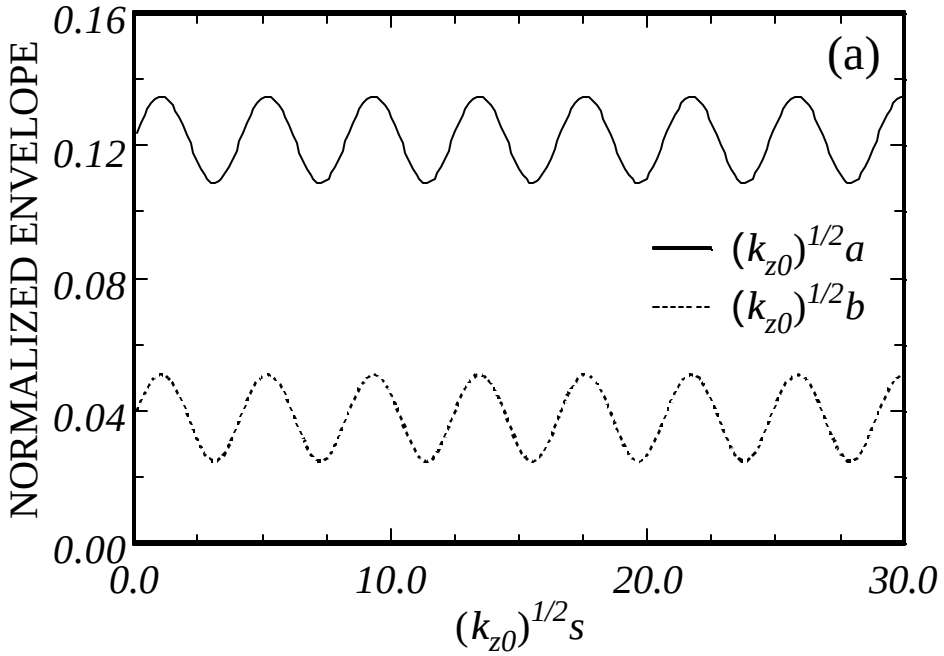
0.16
0.12
0.08
0.04
0.00
NORMALIZED ENVELOPE
(a)
$(k_{z0})^{1/2}a$
$(k_{z0})^{1/2}b$
0.0
10.0
20.0
30.0
$(k_{z0})^{1/2}s$

Fig. 3(a)

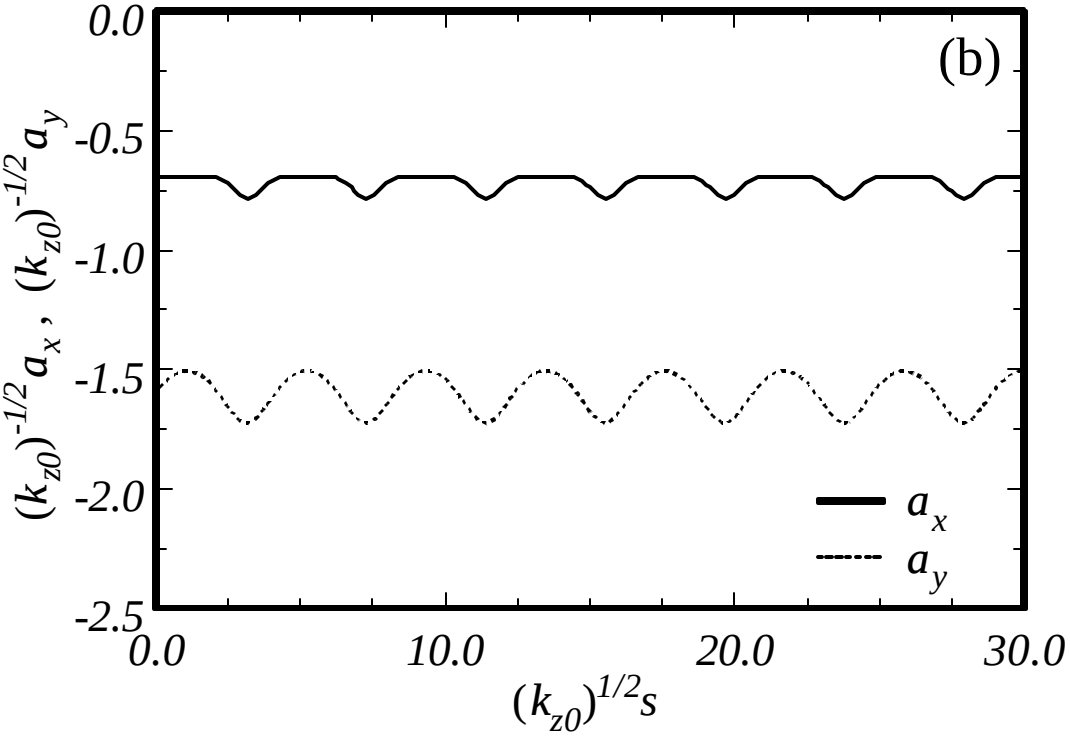

Fig. 3(b)

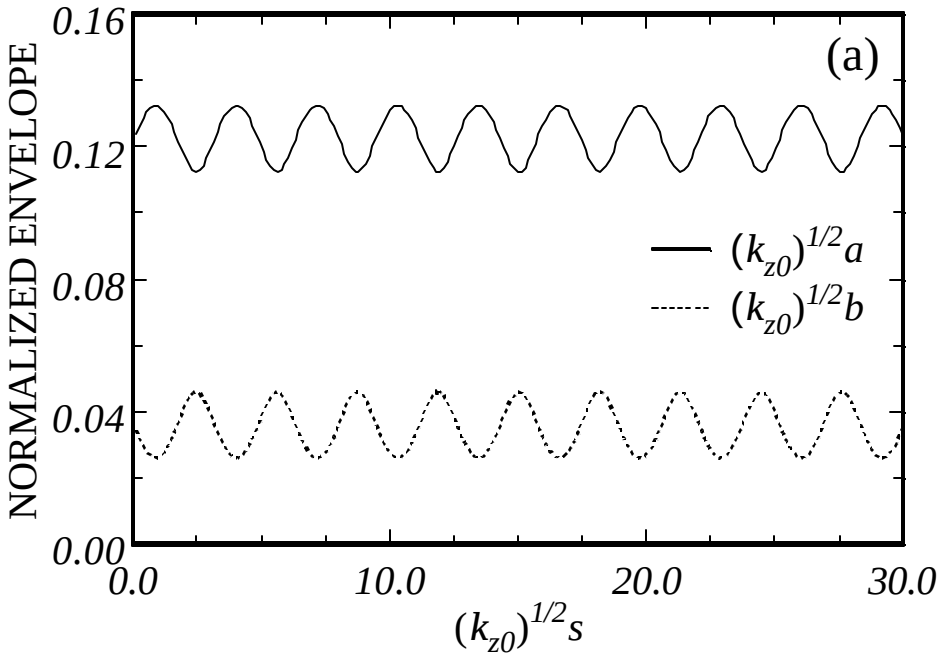
0.16
0.12
0.08
0.04
0.00
NORMALIZED ENVELOPE
(a)
$(k_{z0})^{1/2}a$
$(k_{z0})^{1/2}b$
0.0
10.0
20.0
30.0
$(k_{z0})^{1/2}s$

Fig. 4(a)

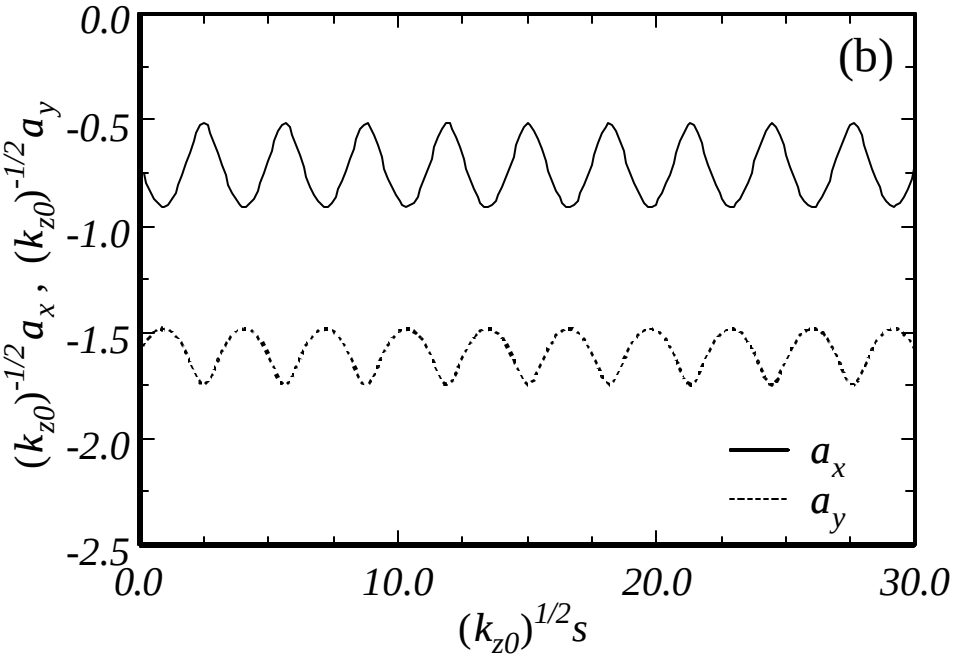

Fig. 4(b)